Best Practice & Research Clinical Endocrinology & Metabolism 33 (2019) 101278

Contents lists available at ScienceDirect

Best Practice & Research Clinical Endocrinology & Metabolism

journal homepage: www.elsevier.com/locate/beem

Modern imaging of pituitary adenomas

Waiel A. Bashari, MSc, MRCP(UK), Clinical Fellow [a, 1],
Russell Senanayake, MSc, MRCP(UK), Clinical Fellow [a, 1],
Antía Fernández-Pombo, MD, Clinical Fellow [a, b, 1],
Daniel Gillett, MSc, Clinical Scientist [c],
Olympia Koulouri, MRCP(UK), Clinical Fellow [a],
Andrew S. Powlson, MRCP(UK), Consultant Endocrinologist [a],
Tomasz Matys, PhD, FRCR, Consultant Neuroradiologist [d],
Daniel Scoffings, FRCR, Consultant Neuroradiologist [d],
Heok Cheow, FRCR, Consultant Radiologist [c, d],
Iosif Mendichovszky, PhD, FRCR, Consultant Radiologist [c, d],
Mark Gurnell, PhD, FRCP, Professor of Clinical Endocrinology [a, *]

[a] *Cambridge Endocrine Molecular Imaging Group, Metabolic Research Laboratories, Wellcome Trust-MRC Institute of Metabolic Science, University of Cambridge, National Institute for Health Research Cambridge Biomedical Research Centre, Addenbrooke's Hospital, Hills Road, Cambridge, CB2 0QQ, UK*
[b] *Division of Endocrinology and Nutrition, University Clinical Hospital of Santiago de Compostela, Spain*
[c] *Cambridge Endocrine Molecular Imaging Group, Department of Nuclear Medicine, University of Cambridge, National Institute for Health Research Cambridge Biomedical Research Centre, Addenbrooke's Hospital, Hills Road, Cambridge, CB2 0QQ, UK*
[d] *Cambridge Endocrine Molecular Imaging Group, Department of Radiology, University of Cambridge, National Institute for Health Research Cambridge Biomedical Research Centre, Addenbrooke's Hospital, Hills Road, Cambridge, CB2 0QQ, UK*

ARTICLE INFO

Article history:
Available online 28 May 2019

Keywords:
pituitary
MRI
CT

Decision-making in pituitary disease is critically dependent on high quality imaging of the sella and parasellar region. Magnetic resonance imaging (MRI) is the investigation of choice and, for the majority of patients, combined T1 and T2 weighted sequences provide the information required to allow surgery, radiotherapy (RT) and/or medical therapy to be planned and long-term outcomes to be monitored. However, in some cases standard clinical MR sequences are indeterminate and additional information is

* Corresponding author. Metabolic Research Laboratories, Wellcome Trust-MRC Institute of Metabolic Science, University of Cambridge, Box 289, Addenbrooke's Hospital, Hills Road, Cambridge, CB2 0QQ, UK. Fax: +44 1223 330598.
E-mail address: mg299@medschl.cam.ac.uk (M. Gurnell).
[1] contributed equally to the manuscript.

https://doi.org/10.1016/j.beem.2019.05.002

PET
functional imaging
molecular imaging

needed to help inform the choice of therapy for a pituitary adenoma (PA). This article reviews current recommendations for imaging of PA, examines the potential added value that alternative MR sequences and/or CT can offer, and considers how the use of functional/molecular imaging might allow definitive treatment to be recommended for a subset of patients who would otherwise be deemed unsuitable for (further) surgery and/or RT.

Introduction

Although almost always benign, pituitary adenomas (PA) can be associated with significant morbidity and even increased mortality by virtue of hormone hypersecretion (e.g. acromegaly, Cushing syndrome), hypopituitarism, and local mass effects (e.g. visual loss due to chiasmal compression). Recent studies indicate a prevalence rate that is 3.5 to 5-times higher than previously suspected, with clinically-apparent tumours affecting between 1:1000 and 1:1500 of the general population [1]. It is possible this still represents an under-estimate bearing in mind up to 14.4% (in autopsy studies) and up to 22.5% (in radiologic studies) of the population have been reported to have a pituitary abnormality, but not all of these undergo formal endocrine assessment [2].

In recent years, the repertoire of medical therapies available for the management of pituitary tumours has increased significantly [e.g. the advent of GH receptor (GHR) antagonist or 2nd generation somatostatin receptor ligand (SRL) therapy for acromegaly] [3]. In addition, modern radiotherapy techniques (including stereotactic radiosurgery) allow for more precise targeting of a pituitary adenoma while sparing surrounding structures. However, for many patients pituitary surgery remains an important, often first, step in their management (either with curative intent or to reduce tumour bulk and facilitate more effective adjunctive treatment). Good quality imaging of the sella and parasellar regions is therefore critical to decision-making, even when surgery and/or radiotherapy are not recommended. For most patients, this means undergoing dedicated pituitary magnetic resonance (MR) imaging (MRI), which provides important information about the adenoma itself and key surrounding structures. In a small number of cases, pituitary computed tomography (CT) is required (most commonly when MRI is not possible/tolerated). However, while MRI and/or CT provide sufficient information for the management of the majority of cases, routine clinical sequences do not always reliably identify the site of *de novo*, persistent or recurrent adenoma, which in turn may reduce the opportunity for curative surgery and/or radiotherapy (RT).

Accordingly, several groups have explored the potential utility of using alternative MR sequences to inform the management of different pituitary tumour subtypes. In addition, we and others have examined the role(s) of functional imaging (e.g. using molecular PET tracers), in combination with MRI, to allow more accurate localisation of the site(s) of PA. This article provides an update on current approaches to imaging in pituitary adenomas, reviews possible indications for adopting specific MR (and/or CT) sequences and considers how advances in molecular PET imaging might be used to improve patient outcomes from targeted therapies such as (repeat) transsphenoidal surgery (TSS) or stereotactic radiosurgery (SRS).

Magnetic resonance imaging

MRI is the preferred cross-sectional imaging modality for identifying lesions within the pituitary gland and surrounding parasellar region, and provides a high detection accuracy [4–6]. When requesting a pituitary MR scan, several factors should be taken into account (Table 1).

The normal anterior pituitary gland is isointense to grey matter on non-contrast T1 and T2 weighted standard Spin Echo (SE) sequences (Fig. 1a,b,e,f), while the posterior pituitary has intrinsic high T1 signal (Fig. 1b) but is hypointense on T2. Following contrast injection, the infundibulum and gland

Table 1
Points to consider when requesting a pituitary MRI protocol.

Key questions	Options/examples
Which sequences?	Spin Echo (SE)/Fast Spin Echo (FSE): - T1 weighted[1,2] - T2 weighted - proton density (PD) weighted[2] Gradient Echo (GE): - spoiled gradient echo (e.g. to permit thinner slices through the sella – see below) Other: - Diffusion weighted (DWI) - Perfusion weighted (PWI) - Inversion recovery (IR) - Fluid attenuation inversion recovery (FLAIR) - Magnetic resonance angiography (MRA)
With or without contrast enhancement?	Gadolinium[1]
Which planes?	Coronal; sagittal; axial
Which slice thickness?	Standard 2–3 mm; volumetric (e.g. consecutive 1 mm)
Which magnetic field strength?	1.5T, 3T, 7T

Key: [1]T1 weighted MRI following contrast may also include (i) ***dynamic sequences*** [images obtained from multiple locations throughout the gland at multiple time points (e.g. 0, 30, 60, 90, 120 and 180 s) to help identify microadenomas (which exhibit delayed enhancement) or distinguish residual/recurrent tumour from postoperative change], and (ii) ***delayed sequences*** (to assess the cavernous sinuses and characterize other sella/parasellar tumours). [2]Fat suppressed T1 or PD sequences may improve visualization of the posterior pituitary gland by suppressing signal from adjacent clival bone marrow.

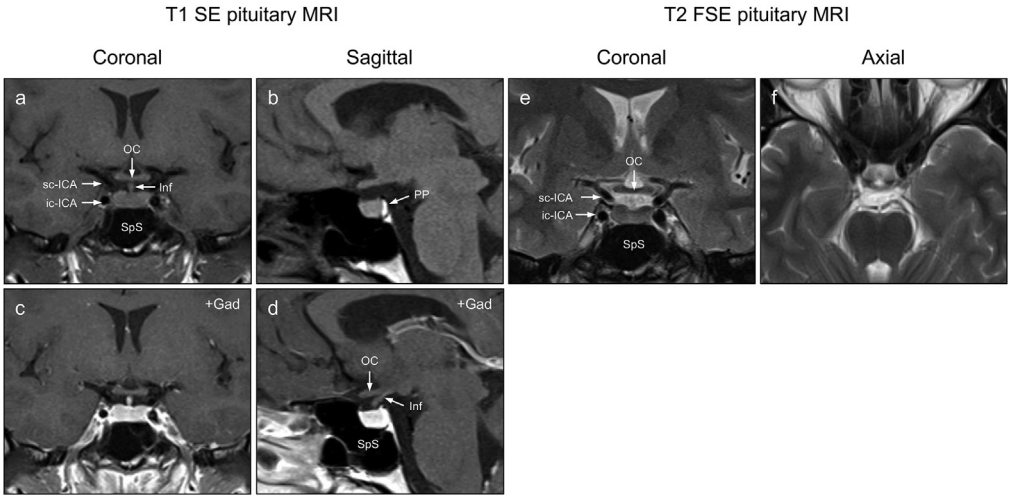

Fig. 1. Normal pituitary MRI. **a-d** Spin Echo (SE) T1 weighted coronal and sagittal sequences (pre- and post-gadolinium enhancement). **e,f** Fast Spin Echo (FSE) T2 weighted coronal and axial sequences. ***Key:*** Gad, gadolinium; ic-ICA, intracavernous segment of the internal carotid artery; Inf, infundibulum; OC, optic chiasm; PP, posterior pituitary gland; sc-ICA, supracavernous segment of the internal carotid artery; SpS, sphenoid sinus.

progressively enhance (Fig. 1c and d); however, contrast uptake by pituitary adenomas is typically slower, giving rise to delayed enhancement and washout characteristics, which can help to reveal an otherwise poorly visualised microadenoma (Fig. 2a). Gadolinium, a naturally-occurring lanthanide, is the most commonly employed contrast agent during pituitary imaging. It is particularly suited for use

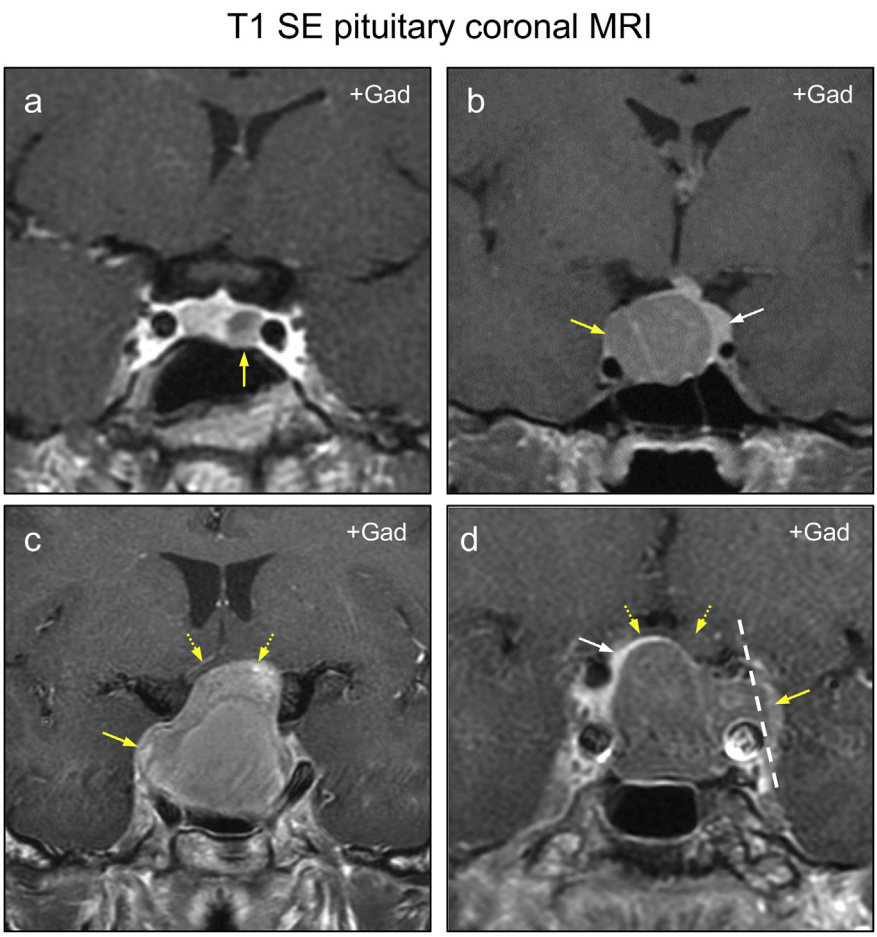

Fig. 2. Spectrum of pituitary adenomas. **a** Left-sided microadenoma exhibiting delayed contrast enhancement (yellow arrow). **b** macroadenoma, displacing the pituitary stalk and normal remaining gland to the left (white arrow); there is only limited suprasellar extension (without compression of the optic chiasm), but clear extension in to the right cavernous sinus (yellow arrow). **c** macroadenoma with marked suprasellar extension compressing the optic chiasm (left > right) (dotted yellow arrows) and right parasellar extension (yellow arrow). **d** macroadenoma with suprasellar extension resulting in compression of the optic chiasm (dotted yellow arrows) and left parasellar extension (yellow arrow) – Knosp grade 3A (white dashed line); the remaining normal gland is seen on the right/superiorly (white arrow). ***Key:*** Gad, gadolinium; T1 SE, T1 weighted Spin Echo MRI.

as an MRI contrast agent because it has seven unpaired electrons which confer strong paramagnetic properties. In its free form Gadolinium is toxic and it must therefore be chelated to a carrier ligand to allow clinical use. Gadolinium-based contrast agents (GBCAs) can be divided in to four groups according to whether the carrier ligand is linear or macrocyclic and ionic or non-ionic. In recent years concern has been raised regarding the safety of GBCAs, and the pituitary community has been alerted to the potential for long-term central nervous system retention even in patients with normal renal function, which is particularly relevant given the need for many pituitary patients to continue with long-term imaging surveillance [7]. Macrocyclic GBCAs exhibit greater chemical stability than their linear counterparts, and this has been linked to a lower risk of nephrogenic systemic fibrosis and reduced gadolinium tissue deposition; however, they appear to carry a higher risk of allergic reactions,

albeit still relatively rare. Therefore, while GBCAs continue to play an important role in imaging of the sella and parasellar region, it is important to consider when contrast might not be required [e.g. when T1 non-contrast and/or T2 sequences alone can provide sufficient information to inform management (see below)], thereby minimising exposure [8].

Another important consideration when imaging the sella is the choice of magnetic field strength. 1.5T SE MRI is still commonly used in routine clinical practice and provides reasonable spatial resolution to permit 2.0 mm or 3.0 mm slice thickness. However, very small microadenomas (e.g. Cushing, thyrotropinoma) may escape detection, although this risk can be partially mitigated by careful selection of the T1 SE parameters [9]. In recent years, higher field strength MRI systems (3T and more latterly 7T) have become available, providing higher signal to noise ratio with a reduction in acquisition time, and allowing 1.0 mm sections to be performed [10–12]. Therefore, while 1.5T SE MRI is a reasonable option in the first instance, for those patients with suspected microadenomas but with equivocal or 'negative' 1.5T scans, referral for a 3T study should be considered [13]. However, it remains to be seen whether using 7T MRI brings sufficient additional benefits to outweigh potential challenges such as the identification of a greater number of incidental pituitary abnormalities.

In routine clinical practice, most PA are readily visualised on T1 and T2 weighted MRI which provide important information about the size of the lesion [micro- (<1 cm) versus macro- (≥1 cm) adenoma] and the degree of parasellar involvement (Fig. 2). Several approaches have been proposed to define the extent of lateral extension and cavernous sinus invasion, with the most commonly used being the Knosp classification [14]. As a general rule, the higher the grade, the greater the degree of cavernous sinus involvement, and the lower the probability of achieving full surgical remission. The inclusion of Grades 3A and 3B differentiates between the different outcomes for adenomas invading the superior and the inferior cavernous sinus compartments (Fig. 2d) [15].

Dynamic contrast-enhanced MRI (based on T1 weighted images obtained pre-and immediately following gadolinium injection) (Table 1) may be indicated when standard sequences have failed to identify a pituitary lesion but clinical features strongly suggest the presence of an adenoma, for example in suspected Cushing disease due to an ACTH-secreting microadenoma [5,16]. However, gradient echo [e.g. spoiled gradient echo (SGE)/(fast) spoiled gradient recalled echo (FSPGR/SPGR)] has been reported to offer greater sensitivity for detecting corticotroph microadenomas with only occasional cases detected on dynamic but not gradient echo MRI [16]. Strategies such as the administration of corticotrophin-releasing hormone immediately prior to scanning have not provided convincing evidence of an additional benefit [13].

Recently, there has been a resurgence of interest in the potential added value that T2 sequences can offer when assessing pituitary lesions – in particular, offering diagnostic insights that are not deducible from T1 sequences, and also potentially sparing the need for contrast enhanced imaging in some patients (thus reducing GBCA exposure – see above). Jean-François Bonneville has elegantly made the

Table 2
Specific indications for T2 weighted pituitary MRI – according to Bonneville [8].

Indication	T2 weighted MRI findings	References
Suspected microprolactinoma - potential to obviate requirement for gadolinium injection	Hyperintense	[8]
Identification of silent corticotroph macroadenomas – with differentiation from non-functioning PA	Microcystic pattern (in >50% of cases)	[8,48]
Investigation of GH-secreting PA: - prediction of response to first generation SSA therapy - identification of invasion of the medial wall of the cavernous sinus	Hypointense [commoner (>50%)]: smaller tumours with less CSI, which correspond to densely granulated tumours; good response to SSA Isointense/hyperintense: larger, typically more invasive tumours; less SSA responsive	[8,49,50]
Diagnosis of hypophysitis	Hyperintense (even when overall size of gland is within normal limits)	[8]
Diagnosis of Rathke's cleft cyst	Hypointense	[8]

Key: CSI, cavernous sinus invasion; PA, pituitary adenoma; SSA, somatostatin analogue therapy.

case for increased use (and reporting in the literature) of T2 MR findings in several pituitary disorders, and these are summarised in Table 2 [8].

An array of alternative MR sequences, which are routinely employed in other clinical contexts, have also been tried in several pituitary disorders with mixed results (Table 3). Although several have shown

Table 3
Alternative MR sequences that have been applied in the investigation of pituitary disorders.

MRI sequence	Features	Potential application(s) in pituitary disorders	References
Diffusion weighted (DWI)	Measures the diffusion of water molecules in biological tissues; most commonly used to detect cytotoxic oedema in the context of acute cerebral ischaemia/infarction	Detection of acute pituitary apoplexy/ infarction	[51]
		Distinguishing intra-/supra-sellar cystic lesions	[52]
Apparent Diffusion Coefficient (ADC)	A subtype of DWI	Prediction of the consistency of PA pre-surgery:	
		- some authors have reported a reduced ADC with increasing collagen content	[53–55]
		- others have found no relation between ADC and tumour consistency	[56–58]
Diffusion Tensor (DTI)	An extension of DWI which analyses the directional diffusion of water molecules in biological tissue	Optic nerve tractography to inform treatment planning and predict likelihood of visual recovery following transsphenoidal surgery	[59–61]
Perfusion weighted (PWI)	Assesses tissue perfusion at the capillary level	Assessment of the vascularity of PA pre-surgery	[62]
		Identification of other vascular lesions (e.g. meningioma) which may be mistaken for a PA	[63,64]
Magnetic Resonance Angiography (MRA)	Provides detailed images of the arterial system	Detection of intrasellar aneurysms	[65]
		Delineation of cranial nerves in their cavernous sinus segment	[66]
Magnetic Resonance Elastography (MRE)	Measures the propagation of shear waves through tissue of interest to provide an estimate of stiffness	Inform surgical planning by estimating whether a PA is likely to be soft (and suckable), or intermediate or firm (requiring curettage for resection)	[67]
Magnetic Resonance Spectroscopy (MRS)	Provides information on metabolic function through the measurement of different metabolites (e.g. acetylaspartate, choline, creatine)	Differentiation of PA from normal gland	[68]
		Differential diagnosis of suprasellar lesions	[69,70]
		Predicting response of somatotroph tumours to SSA therapy	[71]
Balanced steady state free precession (e.g. Constructive Interference in Steady State, CISS; Fast Imaging Employing Steady-state Acquisition Cycled phases, FIESTA-C)	Image contrast determined by T2/T1 ratio of the tissue; in practice, heavily water weighted (good contrast between CSF and other structures) but also sensitive to contrast enhancement	Improved detection of adenoma in Cushing disease	[72]
		Improved evaluation of cavernous sinus invasion	[72]
		Prediction of adenoma consistency	[73]
		Improved delineation of optic nerves and chiasm in large pituitary tumors	[74]
Fluid Attenuation Inversion Recovery (FLAIR)	An inversion recovery sequence with a long inversion time that removes signal from the CSF which is therefore dark rather than bright as would normally be seen on T2 sequences	In Cushing disease, delayed contrast washout from a corticotroph microadenoma may be detected as FLAIR hyperintensity	[75]

Key: PA, pituitary adenoma; SSA, somatostatin analogue therapy.

potential promise, for the most part findings need confirmation in larger cohorts before they can be recommended for routine clinical use.

Computed tomography (CT)

Modern computed tomography (CT) is a reasonable substitute where MRI is contraindicated (including in patients with non-MR compatible pacemakers/cardiac devices, vascular clips or metallic foreign bodies) or when the patient declines MRI (e.g. due to claustrophobia). Reasonable evaluation of pituitary macroadenomas is possible with dedicated pituitary CT (Fig. 3a), but it is generally less informative for the assessment/detection of small tumours, although advanced CT techniques (e.g. dynamic contrast-enhanced multisection CT) have been trialled and may even aid the detection of conventional MR imaging-occult pituitary microadenomas [17].

Even when MRI is possible, there are several situations in which CT can provide useful additional information regarding a sella-based or parasellar lesion. These include identification of bone destruction (e.g. by an invasive macroprolactinoma) (Fig. 3b) and confirmation of suspected intra/parasellar calcification [e.g. calcified PA (with thyrotropinoma being the classic example) or craniopharyngioma] (Fig. 3c). CT is also used in conjunction with MRI to facilitate radiotherapy planning and may reveal previously unsuspected tumour invasion of bony structures [18,19].

Functional pituitary imaging

Despite recent advances in cross-sectional imaging, there remain several situations in which clinical decision-making is limited by indeterminate MRI and/or CT findings, including:

(i) small PA that cannot be readily visualised even using a combination of sequences (e.g. corticotroph adenomas may evade detection in 30–40% of patients with Cushing disease [20]; similarly, thyrotroph and lactotroph tumours are not always easily localised)
(ii) following primary intervention (surgery, radiotherapy or medical therapy) when post-treatment change may be difficult to distinguish from residual functioning tumour
(iii) in the presence of a confounding pituitary incidentaloma

Functional imaging represents an alternative and complementary approach to traditional anatomical imaging and has found widespread use in many endocrine disorders [e.g. technetium-99m-pertechnetate and technetium-99m-sestamibi scintigraphy in hyperthyroidism and hyperparathyroidism respectively; ^{123}I-metaiodobenzylguanidine (^{123}I-MIBG) scintigraphy for detection of

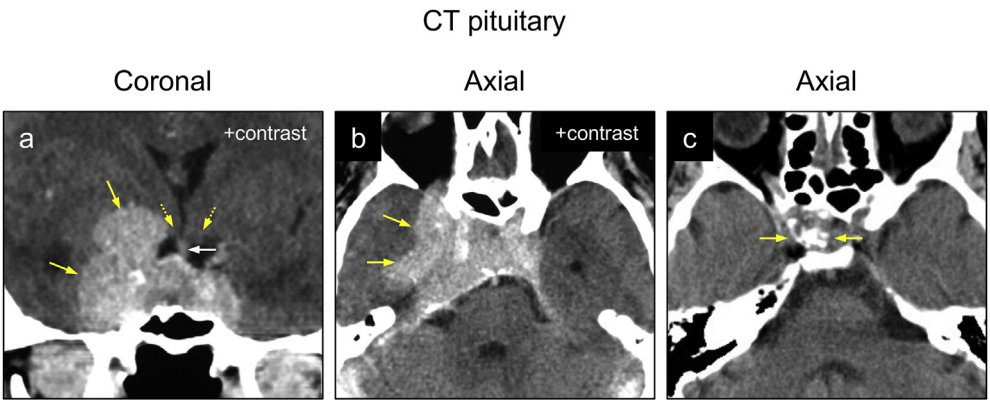

Fig. 3. Pituitary CT. **a,b** Macroprolactinoma with extensive right parasellar and suprasellar extension, and involvement of the skull base (yellow arrows); the position of the optic chiasm (yellow dotted arrows) and infundibulum (white arrow) are shown. **c** Intrasellar calcification (yellow arrows) in a patient with a thyrotroph adenoma.

phaeochromocytoma/paraganglioma]. However, while scintigraphy remains a useful clinical technique, especially when combined with single photon emission computed tomography (SPECT) for image acquisition, its application in other fields of endocrinology has been limited by its modest sensitivity for detecting small lesions.

Positron emission tomography (PET) offers a solution to this problem and can be combined with CT (PET/CT) or MRI (PET/MR) to allow detection of even subcentimetre lesions. The development of PET ligands targeting different cellular processes (e.g. glucose or amino acid uptake, receptor or intracellular enzyme expression) has opened up new opportunities for the application of PET in endocrine disorders. The potential superiority of PET over conventional scintigraphy is exemplified by the comparison of ^{111}Indium-pentetreotide scintigraphy (±SPECT) ('octreoscan') and ^{68}Gallium-DOTATATE PET/CT for the investigation of neuroendocrine tumours (NET), where the latter often detects lesions not seen on a conventional octreoscan [21].

To date, functional imaging has found limited use in the routine management of pituitary adenomas, although several groups have explored various modalities including somatostatin receptor scintigraphy or PET, ^{18}F-fluorodeoxyglucose (18F-FDG)-PET and ^{11}C-methionine (^{11}C-Met)-PET.

Somatostatin receptor scintigraphy and PET

Somatostatin receptors (SSTRs) are expressed in normal human pituitary tissue and, to varying degrees, in different subtypes of pituitary adenoma. For example, somatostatin receptor subtype 2 (SSTR2) is detectable in most somatotroph adenomas, whereas SSTR5 expression is more variable [22]. In contrast, corticotroph adenomas express higher levels of SSTR3 and SSTR5, but have also recently been confirmed to express SSTR2A [23]. The use of Somatostatin Receptor Scintigraphy (e.g. ^{111}Indium-pentetreotide) in the investigation and management of PA is therefore confounded by several factors: background uptake by normal pituitary tissue; dependence on SSTR subtype expression of the tumour; and limited spatial resolution and sensitivity of scintigraphy, even when combined with SPECT. ^{68}Ga-DOTATATE PET has the potential to address the latter, but it has yet to find clear utility in the management of PA, although preliminary data suggests that combination with ^{18}F-FDG PET may allow distinction of normal gland and adenoma in some cases of primary and recurrent disease [24,25].

^{18}F-FDG PET

The literature contains numerous case reports of incidentally-detected ^{18}F-FDG uptake by pituitary adenoma [26–29]. In contrast, in a large retrospective analysis of incidental pituitary uptake in >40,000 patients who had undergone whole body FDG PET/CT, the overall incidence was just 0.073% [30]. Together these findings (demonstrable uptake by PA with a negligible false positive rate) suggest a possible role for ^{18}F-FDG PET in pituitary imaging. Indeed, the potential utility of ^{18}F-FDG PET has been explored in various subtypes of PA [24,25]. But has been most extensively studied in the context of corticotroph tumours, which often evade detection on MRI. However, findings have been largely disappointing. In a prospective study of ten consecutive patients with subsequently confirmed CD, high resolution ^{18}F-FDG PET (^{18}F-FDG hrPET) was performed together with SE and SPGR MRI [31]. ^{18}F-FDG hrPET revealed increased tracer uptake in four patients, two of whom had no demonstrable lesion on SE MRI. However, SPGR proved more sensitive than ^{18}F-FDG hrPET, identifying a pituitary adenoma in seven cases and, importantly, no adenomas were detected by ^{18}F-FDG hrPET that were not visualised on SPGR MRI. A comparable detection rate (58%) was reported by Alzahrani and colleagues in their retrospective study of 12 patients who underwent conventional ^{18}F-FDG PET/CT [32]. Accordingly, ^{18}F-FDG PET has yet to find a place in the routine management of PA.

^{11}C-methionine PET

Several groups have demonstrated the potential utility of ^{11}C-methionine PET/CT (Met-PET/CT) in different pituitary tumour subtypes, both for the localisation of *de novo* tumours, especially microadenomas, and also for the identification of persistent or recurrent disease [18,33–36]. However, a key limitation of Met-PET/CT is the relative lack of anatomical detail provided by CT when compared with

MRI. This has led us and other workers to explore the possibility of fusing functional images derived from PET-CT with cross-sectional images obtained during volumetric MRI (e.g. FSPGR MRI) [35–38]. In this way, the precise site(s) of ^{11}C-methionine uptake can be delineated through coregistration of PET/CT and MRI images. With the advent of PET/MR this process will become even easier and more convenient, as has been demonstrated with other tracers [25].

However, several important considerations must be taken in to account when developing a specialist pituitary imaging service using ^{11}C-methionine PET.

Patient selection and preparation

Careful case selection is important. The majority of patients with PA do not require molecular imaging. However, the ability to correlate structure with function is potentially useful when either a small *de novo* functioning tumour (e.g. in Cushing disease, thyrotropinoma, prolactinoma or, less

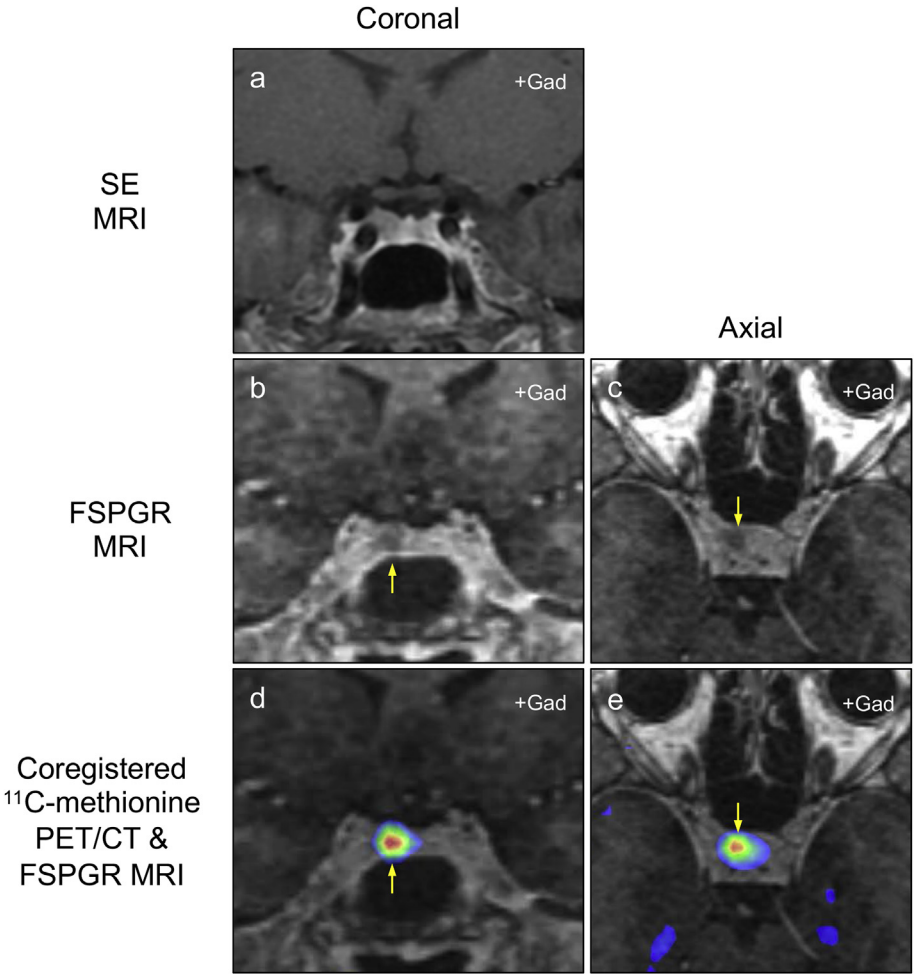

Fig. 4. Confirmation of suspected microprolactinoma using ^{11}C-methionine PET. **a** Indeterminate coronal T1 weighted gadolinium enhanced SE MRI in a 22-year-old female with bilateral galactorrhoea, secondary amenorrhoea and moderate hyperprolactinaemia (PRL 3.8 × upper limit of normal), confounded by antipsychotic medication usage. **b,c** Post-gadolinium FSPGR MRI in coronal and axial planes identifies a possible right-sided microadenoma (yellow arrows). **d,e** ^{11}C-methionine PET/CT coregistered with FSPGR MRI confirms the site of the suspected microprolactinoma (yellow arrows). ***Key:*** FSPGR, Fast Spoiled Gradient Recalled Echo; Gad, gadolinium; PRL, prolactin; SE, Spin Echo.

commonly, acromegaly), or residual/recurrent functioning PA (e.g. acromegaly) cannot be reliably identified on good quality MRI, and when definitive treatment (TSS or SRS) would otherwise be considered. As molecular imaging with ^{11}C-methionine depends on the presence of functioning adenoma tissue, it is important to ensure adequate washout of agents that might otherwise suppress hormone production by the tumour [e.g. SSA or dopamine agonist (DA) therapy in acromegaly], and to confirm active disease prior to imaging. We recommend discontinuation of short-acting SSA therapy (i.e. octreotide) and DA at least one month prior to scanning. For depot SSA (e.g. Sandostatin LAR® or Lanreotide Autogel®) a longer washout period is required (typically 3 months). Patients should be instructed to fast for at least 4 h before the scan. On the day, a further assessment of disease activity [paired random GH and IGF-1 in acromegaly; paired 9am adrenocorticotrophic hormone (ACTH) and

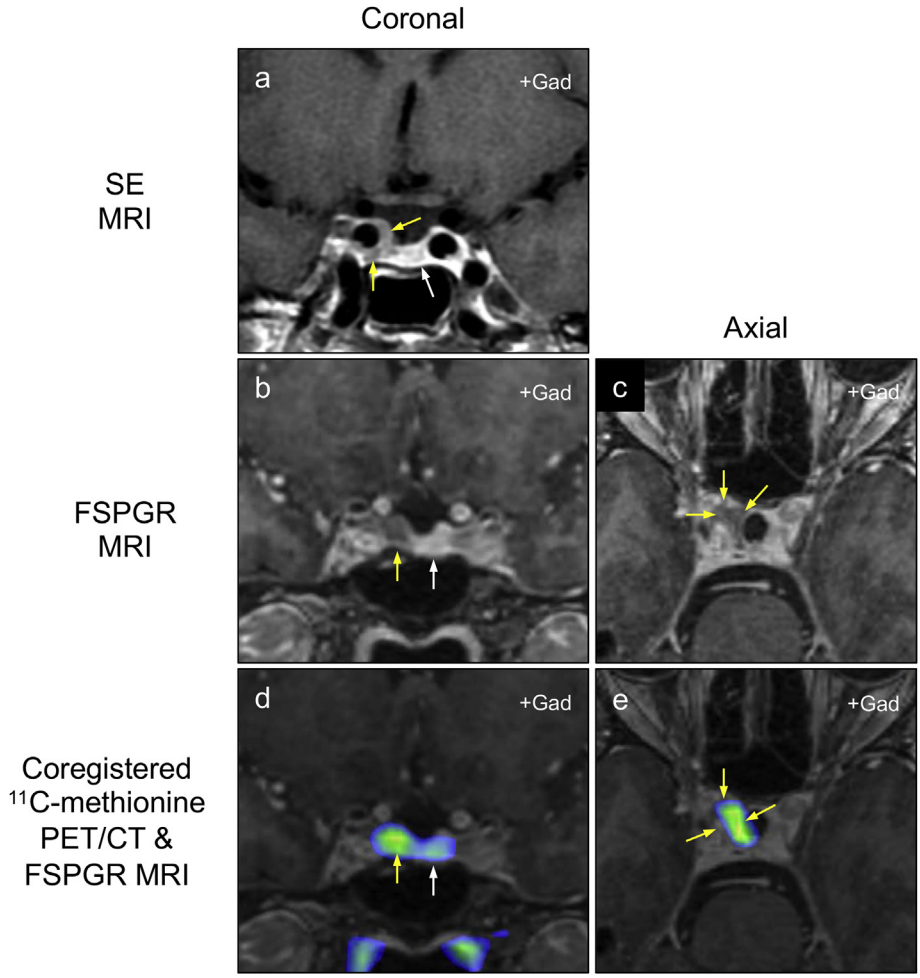

Fig. 5. Confirmation of site of suspected residual somatotroph adenoma using ^{11}C-methionine PET. **a** T1 weighted gadolinium enhanced SE MRI in a 50-year-old female with persistent acromegaly following transsphenoidal surgery (IGF-1 1.9 × upper limit of normal); poorly enhancing tissue can be seen medial and inferior to the right cavernous sinus (yellow arrows), with normal enhancing tissue on the left of the sella (white arrow). **b,c** Post-gadolinium FSPGR MRI in coronal and axial planes confirms an area of poorly enhancing tissue on the right of the sella possibly extending in to the right cavernous sinus (yellow arrows). **d,e** ^{11}C-methionine PET/CT coregistered with FSPGR MRI demonstrates focal tracer uptake in the right side of the sella, but without cavernous sinus extension (yellow arrows); note low level tracer uptake is also seen in the residual normal pituitary tissue (white arrow). ***Key:*** FSPGR, Fast Spoiled Gradient Recalled Echo; Gad, gadolinium; IGF-1, insulin-like growth factor 1; SE, Spin Echo.

cortisol followed by late night salivary cortisol in Cushing syndrome; paired free thyroxine and TSH in thyrotropinoma; prolactin in prolactinoma], together with assessment of remaining pituitary function, should be undertaken.

Tracer production

Carbon-11 (^{11}C) has a half-life of just 20 min and is synthesised using a particle accelerator (Cyclotron). Following production, several quality control steps (identification, purity, stability, half-life confirmation, pH detection and substance sterility) must be completed before the tracer can be administered [39]. The short half-life therefore limits its use to centres with an in-house cyclotron. Typically, between 100 and 400 MBq is administered intravenously.

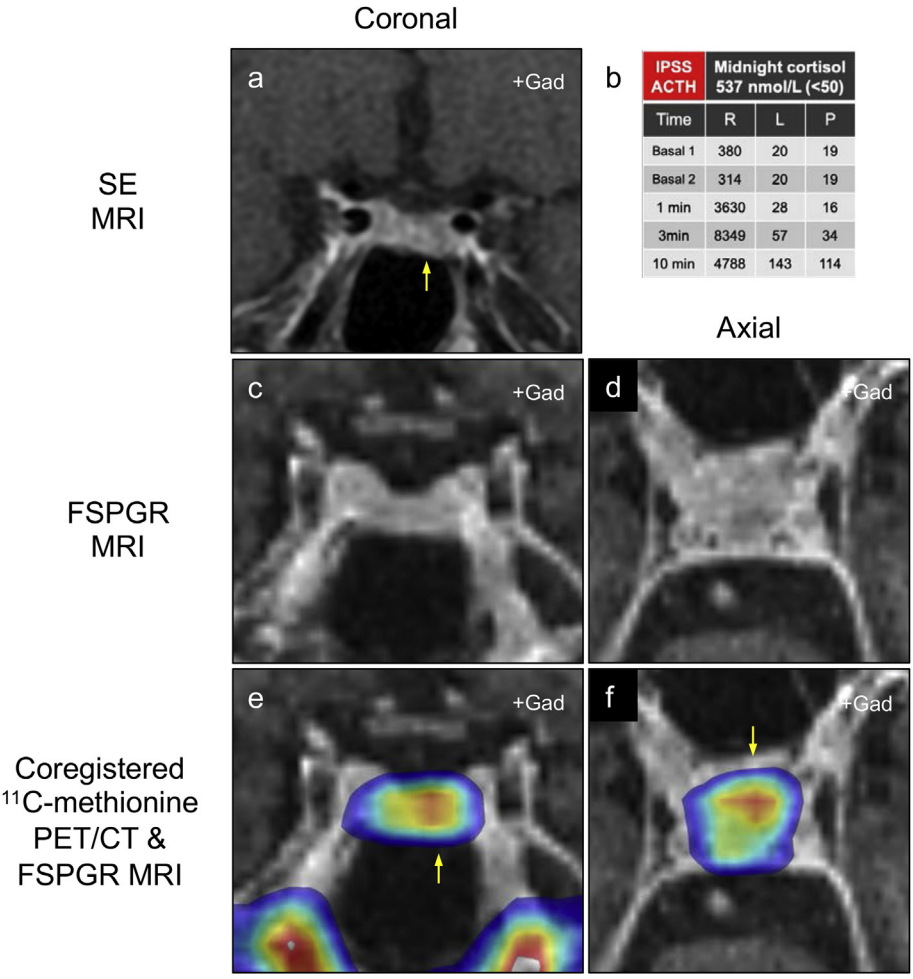

Fig. 6. Identification of a left-sided corticotroph adenoma using ^{11}C-methionine PET. **a** Indeterminate T1 weighted gadolinium enhanced SE MRI in a 32-year-old female with Cushing disease; there is minor inferior deviation of the floor of the sella on the left (yellow arrow), but no clear adenoma is seen. **b** bilateral inferior petrosal sinus sampling shows clear central:peripheral (>245:1 at 3 min) and right:left (>145:1 at 3 min) ACTH (ng/L) gradients following injection of 100 mcg human CRH **c,d** Post-gadolinium FSPGR MRI in coronal and axial planes fails to identify a definite adenoma. **d,e** ^{11}C-methionine PET/CT coregistered with FSPGR MRI demonstrates focal tracer uptake in the left side of the gland (yellow arrows); at surgery a left-sided corticotroph adenoma was resected with resultant hypocortisolism. ***Key:*** CRH, corticotrophin releasing hormone; FSPGR, Fast Spoiled Gradient Recalled Echo; Gad, gadolinium; L, left; P, peripheral; R, right; SE, Spin Echo.

PET acquisition

Uptake time is typically standardised (e.g. 20 min) following tracer injection. Acquisition of low dose CT images allows for attenuation correction (AC) of the PET dataset. A similar approach is required for hybrid PET/MR systems [40–43].

PET/CT-MRI coregistration

^{11}C-methionine PET/CT coregistration to independently acquired MRI (Met-PET-MRI^{CR}) can be performed using commercially available image fusion software. Amongst the most commonly used are automated (e.g. GE Xeleris®) and manual (e.g. MedCom Prosoma® and Slicer®) systems [44–46]. Volumetric (1 mm thickness) MRI facilitates coregistration.

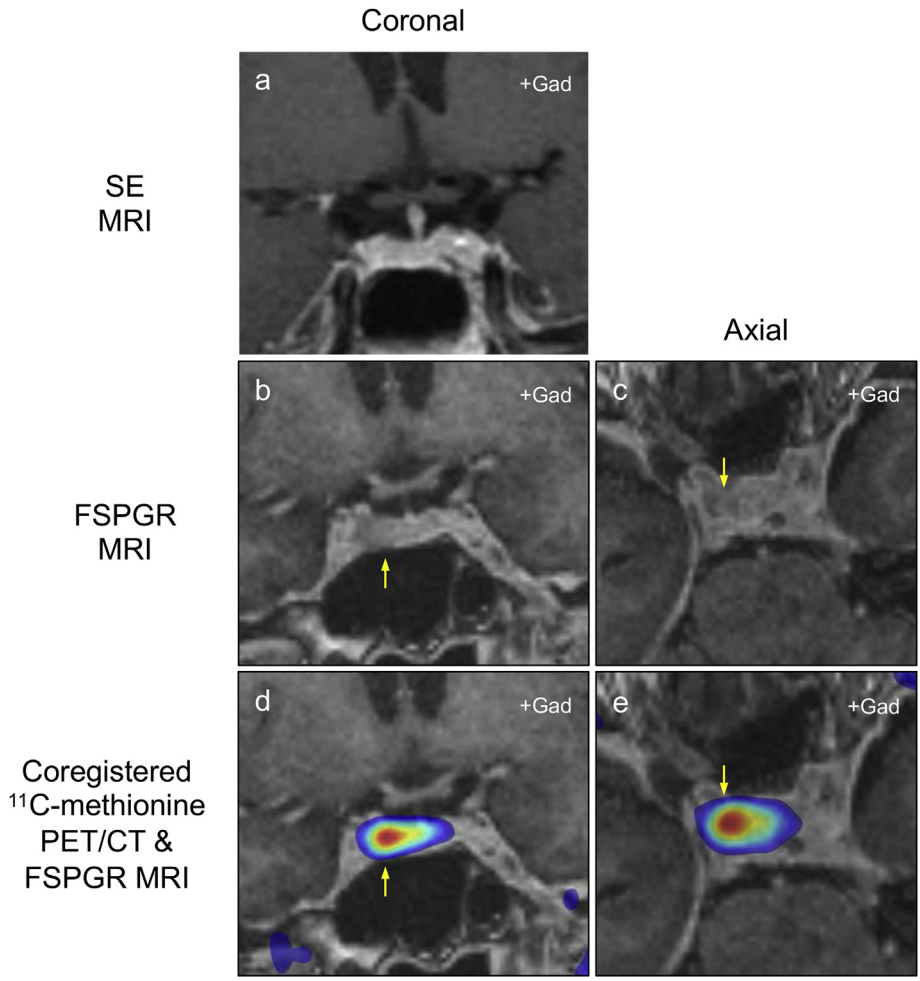

Fig. 7. Identification of a right-sided thyrotroph adenoma using ^{11}C-methionine PET. **a** Indeterminate T1 weighted gadolinium enhanced SE MRI in a 62-year-old female with a biochemically confirmed thyrotropinoma; no clear adenoma is seen. **b,c** Post-gadolinium FSPGR MRI in coronal and axial planes raises suspicion of a possible abnormality on the right side of the sella (yellow arrows), but no definite adenoma is seen. **d,e** ^{11}C-methionine PET/CT coregistered with FSPGR MRI demonstrates intense focal tracer uptake in the right side of the gland (yellow arrows); at surgery a right-sided thyrotroph adenoma was resected with complete resolution of hyperthyroxinaemia secondary to inappropriate TSH secretion. ***Key:*** FSPGR, Fast Spoiled Gradient Recalled Echo; Gad, gadolinium; SE, Spin Echo.

^{11}C-methionine PET/CT-MRI findings in different PA subtypes

Prolactinoma. Lactotroph PA generally demonstrate avid ^{11}C-methionine uptake (up to 9 times background brain uptake). In patients with hyperprolactinaemia for whom medical therapy with DA is not tolerated or advised, and in whom pituitary MRI is indeterminate, Met-PET-MRI^{CR} can facilitate localisation of the tumour to guide selective TSS (Fig. 4). Similarly, in drug resistant macroprolactinomas the site(s) of residual disease can be readily localized to help the pituitary

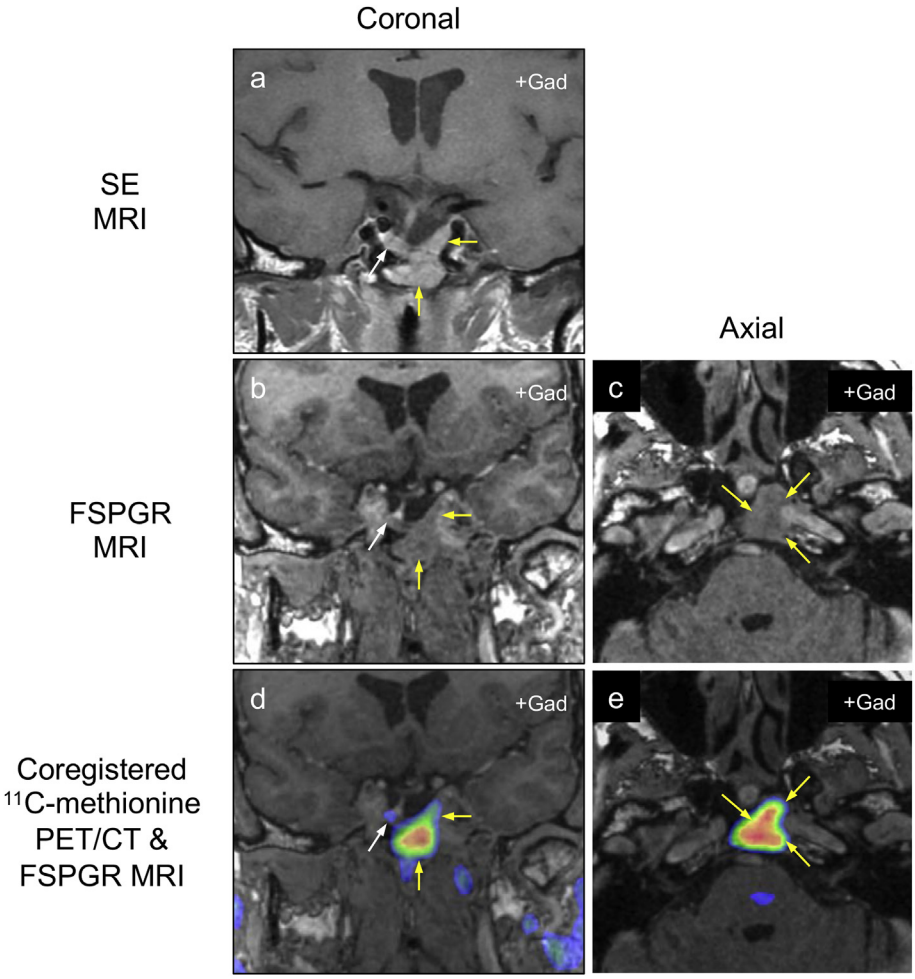

Fig. 8. Confirmation of the site of recurrent gonadotropinoma using ^{11}C-methionine PET. **a** T1 weighted gadolinium enhanced SE MRI in a 50-year-old male with a recurrent functioning FSH-secreting pituitary adenoma; abnormal tissue is seen in the left sella region with extension in to the sphenoid sinus (yellow arrows), but it is difficult to be sure whether this all represents recurrent disease as opposed to post-operative change; the pituitary stalk and normal gland are displaced to the right (white arrow). **b,c** Post-gadolinium FSPGR MRI in coronal and axial planes confirms the findings on SE sequences. **d,e** ^{11}C-methionine PET/CT coregistered with FSPGR MRI demonstrates focal tracer uptake predominantly by tissue in the sphenoid sinus with only modest sella uptake (yellow arrows); the normal gland shows low level uptake of 11C-methionine (white arrow). ***Key:*** FSPGR, Fast Spoiled Gradient Recalled Echo; Gad, gadolinium; SE, Spin Echo.

multidisciplinary team decide whether surgery or RT is appropriate (Bashari, Koulouri and Gurnell, unpublished data).

Acromegaly. Similar to lactotroph tumours, somatotropinomas avidly take up ^{11}C-methionine and Met-PET-MRI^{CR} can help distinguish metabolically active residual/recurrent PA from scar tissue (see Fig. 5) [36]. As indicated above, certain types of medical therapy (e.g. SSA, DA) can diminish tracer uptake and appropriate washout should be completed before imaging is performed [36].

Cushing disease. ^{11}C-methionine uptake by corticotroph adenomas is typically less than is seen in other pituitary tumour subtypes. Possible reasons for this include the relatively low representation of corticotrophs amongst anterior pituitary cells (10–20%); their localization in the centre of the gland

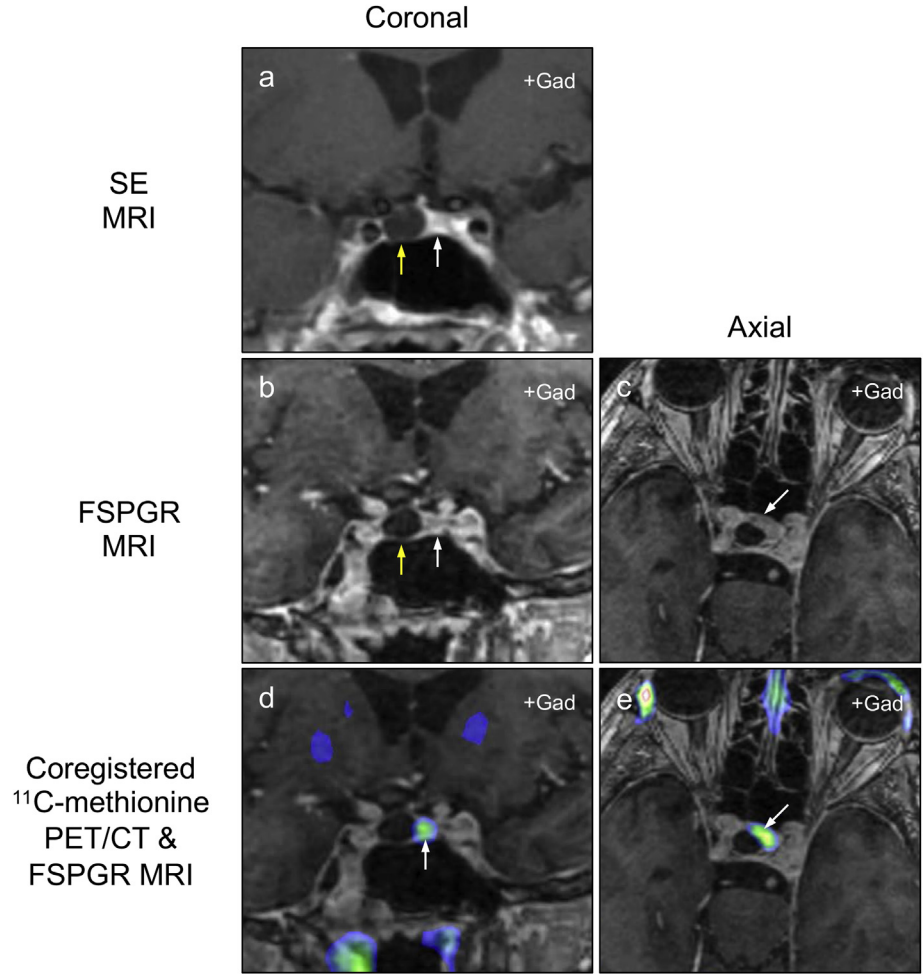

Fig. 9. Absent ^{11}C-methionine uptake in a pituitary cyst. **a** T1 weighted gadolinium enhanced SE MRI in a 74-year-old female with an incidentally detected right-sided pituitary cystic lesion (yellow arrow); the normal gland is seen on the left (white arrow). **b,c** Post-gadolinium FSPGR MRI in coronal and axial planes confirms the findings on SE sequences. **d,e** ^{11}C-methionine PET/CT coregistered with FSPGR MRI demonstrates low level tracer uptake only in the normal gland (white arrows). ***Key:*** FSPGR, Fast Spoiled Gradient Recalled Echo; Gad, gadolinium; SE, Spin Echo.

(leading to additional challenges due to tumoral tracer uptake merging with that of the normal gland); in addition, the periodic/cyclical nature of ACTH production in some corticotroph tumours may result in low uptake if the patient is scanned when the tumour is relatively quiescent (hence the need to confirm active disease at the time of imaging). Accordingly, success rates for localizing *de novo* or recurrent corticotroph tumours are of the order of ~70% (Fig. 6) [35].

TSH-secreting PA (thyrotropinoma). The majority of thyrotroph tumours demonstrate avid uptake of ^{11}C-methionine (Fig. 7). We have also shown that this uptake can be suppressed by SSA therapy, thus providing an 'endocrine switch' which can offer added reassurance when MR findings are unconvincing for the presence of an adenoma [37].

Clinically non-functioning pituitary adenoma/gonadotropinoma. Clinically non-functioning PAs (NFPA) and functioning gonadotropinomas also demonstrate significant ^{11}C-methionine uptake which can therefore be used as a biomarker of residual/recurrent disease (Fig. 8).

Reassuringly, ^{11}C-methionine uptake by cystic pituitary lesions within the sella is typically low/absent when compared with the normal background pituitary tissue or a PA (Fig. 9).

Summary

In the majority of cases when pituitary imaging is indicated, good quality T1 (±contrast enhancement) and T2 weighted sequences will provide sufficient information to allow effective clinical decision making. For those patients in whom MRI findings are inconclusive, consideration should be given to the use of other MR sequences, but these should only be requested following discussion with the pituitary multidisciplinary team (MDT). When MRI is not possible or tolerated, thin slice pituitary CT is a reasonable alternative, while in other situations it can augment the findings from MRI (e.g. when bony invasion/destruction is suspected). Although functional imaging with molecular PET tracers (e.g. ^{11}C-methionine) is unlikely to find widespread usage, emerging evidence suggests that in a subgroup of patients it may play an important role in facilitating (further) definitive intervention (e.g. TSS or RT), thereby sparing patients and healthcare systems the need for long-term, often expensive, medical therapy. The establishment of a small number of centres with expertise in molecular pituitary imaging may sit comfortably with the recently proposed model for Pituitary Tumor Centres of Excellence (PTCOE) [47].

Practice Points

- All clinicians involved in the management of pituitary patients should have a good understanding of the MR sequences that are routinely used for pituitary imaging in their centre and when to consider alternative MR protocols.
- The decision to request gadolinium-enhanced MR sequences (e.g. T1 weighted with contrast) should include careful consideration of recent concerns raised regarding gadolinium deposition with GBCAs – if in doubt then discuss with the pituitary MDT and consider the use of alternative sequences (e.g. T2 weighted).
- Pituitary CT is indicated when MRI is not possible or tolerated, and when there is concern regarding bone invasion/destruction or intratumoral calcification.
- Functional imaging with the molecular tracer ^{11}C-methionine (Met-PET-MRI^{CR}) can help identify *de novo* or residual/recurrent PA in all tumour subtypes when MRI findings are inconclusive.

Research Agenda

- It remains unclear whether the advent of MR scanners with increased magnetic field strength (e.g. 7T) will bring added benefits that outweigh the potential disadvantages of identifying a greater proportion of confounding incidental pituitary lesions. Further studies are awaited.
- Although several MRI protocols that find routine use in other clinical settings (e.g. DWI, Elastography) have been applied to pituitary imaging with promising results, further studies are needed to determine whether these should be adopted in to routine clinical practice.
- Functional imaging with the molecular tracer ^{11}C-methionine (Met-PET-MRI^{CR} or Met-PET/MRI) shows significant promise for producing a step change in the management of a subgroup of patients with PA. However, challenges remain when handling the raw datasets and collaborative studies drawing on the expertise of colleagues in the applied sciences (mathematics, physics) will likely be required to take image analysis to the next level.

Funding

This work was supported by the UK NIHR Cambridge Biomedical Research Centre (WB, OK, ASP, IM, MG).

Disclosures

None of the authors have anything to disclose.

Acknowledgements

This work was supported by the UK NIHR Cambridge Biomedical Research Centre and by the Evelyn Trust.

References

[1] Vandeva S, Jaffrain-Rea M-L, Daly AF, et al. The genetics of pituitary adenomas. Best Pract Res Clin Endocrinol Metab 2010;24:461–76. https://doi.org/10.1016/j.beem.2010.03.001.
[2] Ezzat S, Asa SL, Couldwell WT, et al. The prevalence of pituitary adenomas. Cancer 2004;101:613–9. https://doi.org/10.1002/cncr.20412.
[3] Sherlock M, Woods C, Sheppard MC. Medical therapy in acromegaly. Nat Rev Endocrinol 2011;7:291–300. https://doi.org/10.1038/nrendo.2011.42.
[4] Elster AD. Modern imaging of the pituitary. Radiology 1993;187:1–14. https://doi.org/10.1148/radiology.187.1.8451394.
[5] Bonneville J-F, Bonneville F, Cattin F. Magnetic resonance imaging of pituitary adenomas. Eur Radiol 2005;15:543–8. https://doi.org/10.1007/s00330-004-2531-x.
*[6] Bonneville J-F. Magnetic resonance imaging of pituitary tumors. Front Horm Res 2016;45:97–120. https://doi.org/10.1159/000442327.
[7] Nachtigall LB, Karavitaki N, Kiseljak-Vassiliades K, et al. Physicians' awareness of gadolinium retention and MRI timing practices in the longitudinal management of pituitary tumors: a "Pituitary Society" survey. Pituitary 2019;22:37–45. https://doi.org/10.1007/s11102-018-0924-0.
*[8] Bonneville J-F. A plea for the T2W MR sequence for pituitary imaging. Pituitary 2019;22:195–7. https://doi.org/10.1007/s11102-018-0928-9.
[9] Chowdhury IN, Sinaii N, Oldfield EH, et al. A change in pituitary magnetic resonance imaging protocol detects ACTH-secreting tumours in patients with previously negative results. Clin Endocrinol (Oxf) 2010;72:502–6. https://doi.org/10.1111/j.1365-2265.2009.03646.x.
[10] Wolfsberger S, Ba-Ssalamah A, Pinker K, et al. Application of three-tesla magnetic resonance imaging for diagnosis and surgery of sellar lesions. J Neurosurg 2004;100:278–86. https://doi.org/10.3171/jns.2004.100.2.0278.
[11] de Rotte AAJ, van der Kolk AG, Rutgers D, et al. Feasibility of high-resolution pituitary MRI at 7.0 tesla. Eur Radiol 2014;24:2005–11. https://doi.org/10.1007/s00330-014-3230-x.
[12] Rutland JW, Padormo F, Yim CK, et al. Quantitative assessment of secondary white matter injury in the visual pathway by pituitary adenomas: a multimodal study at 7-Tesla MRI. J Neurosurg 2019:1–10. https://doi.org/10.3171/2018.9.JNS182022.
[13] Erickson D, Erickson B, Watson R, et al. 3 Tesla magnetic resonance imaging with and without corticotropin releasing hormone stimulation for the detection of microadenomas in Cushing's syndrome. Clin Endocrinol (Oxf) 2010;72:793–9. https://doi.org/10.1111/j.1365-2265.2009.03723.x.

*[14] Knosp E, Steiner E, Kitz K, et al. Pituitary adenomas with invasion of the cavernous sinus space: a magnetic resonance imaging classification compared with surgical findings. Neurosurgery 1993;33:610–7. discussion 617–8.

*[15] Micko ASG, Wöhrer A, Wolfsberger S, et al. Invasion of the cavernous sinus space in pituitary adenomas: endoscopic verification and its correlation with an MRI-based classification. J Neurosurg 2015;122:803–11. https://doi.org/10.3171/2014.12.JNS141083.

*[16] Grober Y, Grober H, Wintermark M, et al. Comparison of MRI techniques for detecting microadenomas in Cushing's disease. J Neurosurg 2018;128:1051–7. https://doi.org/10.3171/2017.3.jns163122.

[17] Kinoshita M, Tanaka H, Arita H, et al. Pituitary-targeted dynamic contrast-enhanced multisection CT for detecting mr imaging–occult functional pituitary microadenoma. Am J Neuroradiol 2015;36:904–8. https://doi.org/10.3174/ajnr.A4220.

[18] Taku N, Koulouri O, Scoffings D, et al. The use of 11carbon methionine positron emission tomography (PET) imaging to enhance radiotherapy planning in the treatment of a giant, invasive pituitary adenoma. BJR Case Reports 2017;3:20160098. https://doi.org/10.1259/bjrcr.20160098.

[19] Minniti G, Osti MF, Niyazi M. Target delineation and optimal radiosurgical dose for pituitary tumors. Radiat Oncol 2016;11:135. https://doi.org/10.1186/s13014-016-0710-y.

[20] Patronas N, Bulakbasi N, Stratakis CA, et al. Spoiled gradient recalled acquisition in the steady state technique is superior to conventional postcontrast spin echo technique for magnetic resonance imaging detection of adrenocorticotropin-secreting pituitary tumors. J Clin Endocrinol Metab 2003;88:1565–9. https://doi.org/10.1210/jc.2002-021438.

[21] Challis BG, Powlson AS, Casey RT, et al. Adult-onset hyperinsulinaemic hypoglycaemia in clinical practice: diagnosis, aetiology and management. Endocr Connect 2017;6:540–8. https://doi.org/10.1530/EC-17-0076.

[22] Nielsen S, Mellemkjær S, Rasmussen LM, et al. Expression of somatostatin receptors on human pituitary adenomas in vivo and ex vivo. J Endocrinol Invest 2001;24:430–7. https://doi.org/10.1007/BF03351043.

[23] Behling F, Honegger J, Skardelly M, et al. High expression of somatostatin receptors 2A, 3, and 5 in corticotroph pituitary adenoma. Int J Endocrinol 2018;2018:1–12. https://doi.org/10.1155/2018/1763735.

*[24] Zhao X, Xiao J, Xing B, et al. Comparison of 68Ga DOTATATE to 18F-FDG uptake is useful in the differentiation of residual or recurrent pituitary adenoma from the remaining pituitary tissue after transsphenoidal adenomectomy. Clin Nucl Med 2014;39:605–8. https://doi.org/10.1097/RLU.0000000000000457.

[25] Wang H, Hou B, Lu L, et al. PET/MRI in the diagnosis of hormone-producing pituitary microadenoma: a prospective pilot study. J Nucl Med 2018;59:523–8. https://doi.org/10.2967/jnumed.117.191916.

[26] Campeau RJ, David O, Dowling AM. Pituitary adenoma detected on FDG positron emission tomography in a patient with mucosa-associated lymphoid tissue lymphoma. Clin Nucl Med 2003;28:296–8. https://doi.org/10.1097/01.RLU.0000057554.55930.05.

[27] Ryu SI, Tafti BA, Skirboll SL. Pituitary adenomas can appear as hypermetabolic lesions in 18F-FDG PET imaging. J Neuroimaging 2010;20:393–6. https://doi.org/10.1111/j.1552-6569.2008.00347.x.

[28] Maffei P, Marzola MC, Musto A, et al. A very rare case of nonfunctioning pituitary adenoma incidentally disclosed at 18F-FDG PET/CT. Clin Nucl Med 2012;37:e100–1. https://doi.org/10.1097/RLU.0b013e3182485217.

[29] Joshi P, Lele V, Gandhi R. Incidental detection of clinically occult follicle stimulating hormone secreting pituitary adenoma on whole body 18-Fluorodeoxyglucose positron emission tomography-computed tomography. Indian J Nucl Med 2011;26:34–5. https://doi.org/10.4103/0972-3919.84611.

[30] Jeong SY, Lee S-W, Lee HJ, et al. Incidental pituitary uptake on whole-body 18F-FDG PET/CT: a multicentre study. Eur J Nucl Med Mol Imaging 2010;37:2334–43. https://doi.org/10.1007/s00259-010-1571-5.

[31] Chittiboina P, Montgomery BK, Millo C, et al. High-resolution(18)F-fluorodeoxyglucose positron emission tomography and magnetic resonance imaging for pituitary adenoma detection in Cushing disease. J Neurosurg 2015;122:791–7. https://doi.org/10.3171/2014.10.JNS14911.

[32] Alzahrani AS, Farhat R, Al-Arifi A, et al. The diagnostic value of fused positron emission tomography/computed tomography in the localization of adrenocorticotropin-secreting pituitary adenoma in Cushing's disease. Pituitary 2009;12:309–14. https://doi.org/10.1007/s11102-009-0180-4.

[33] Feng Z, He D, Mao Z, et al. Utility of 11C-methionine and 18F-FDG PET/CT in patients with functioning pituitary adenomas. Clin Nucl Med 2016;41:e130–4. https://doi.org/10.1097/RLU.0000000000001085.

[34] Muhr C. Positron emission tomography in acromegaly and other pituitary adenoma patients. Neuroendocrinology 2006;83:205–10. https://doi.org/10.1159/000095529.

*[35] Koulouri O, Steuwe A, Gillett D, et al. A role for 11C-methionine PET imaging in ACTH-dependent Cushing's syndrome. Eur J Endocrinol 2015;173:M107–20. https://doi.org/10.1530/EJE-15-0616.

*[36] Koulouri O, Kandasamy N, Hoole AC, et al. Successful treatment of residual pituitary adenoma in persistent acromegaly following localisation by 11C-methionine PET co-registered with MRI. Eur J Endocrinol 2016;175:485–98. https://doi.org/10.1530/EJE-16-0639.

*[37] Koulouri O, Hoole AC, English P, et al. Localisation of an occult thyrotropinoma with 11C-methionine PET-CT before and after somatostatin analogue therapy. Lancet Diabetes Endocrinol 2016;4:1050. https://doi.org/10.1016/S2213-8587(16)30311-4.

[38] Ikeda H, Abe T, Watanabe K. Usefulness of composite methionine–positron emission tomography/3.0-tesla magnetic resonance imaging to detect the localization and extent of early-stage Cushing adenoma. J Neurosurg 2010;112:750–5. https://doi.org/10.3171/2009.7.jns09285.

[39] Kilian K, Pękal A, Juszczyk J. Synthesis of 11C-methionine through gas phase iodination using Synthra MeIPlus synthesis module. Nukleonika 2016;61:29–33. https://doi.org/10.1515/nuka-2016-0007.

[40] Delso G, Gillett D, Bashari W, et al. Clinical evaluation of 11C-Met-avid pituitary lesions using a ZTE-based AC method. IEEE Trans Radiat Plasma Med Sci 2018. https://doi.org/10.1109/TRPMS.2018.2886838. 1–1.

[41] Vandenberghe S, Marsden PK. PET-MRI: a review of challenges and solutions in the development of integrated multimodality imaging. Phys Med Biol 2015;60:R115–54. https://doi.org/10.1088/0031-9155/60/4/R115.

[42] Wagenknecht G, Kaiser H-JJ, Mottaghy FM, et al. MRI for attenuation correction in PET: methods and challenges. Magn Reson Mater Phys Biol Med 2013;26:99–113. https://doi.org/10.1007/s10334-012-0353-4.

[43] Hofmann M, Steinke F, Scheel V, et al. MRI-based attenuation correction for PET/MRI: a novel approach combining pattern recognition and atlas registration. J Nucl Med 2008;49:1875–83. https://doi.org/10.2967/jnumed.107.049353.
[44] Pooler AM, Mayles HM, Naismith OF, et al. Evaluation of margining algorithms in commercial treatment planning systems. Radiother Oncol 2008;86:43–7. https://doi.org/10.1016/j.radonc.2007.11.006.
[45] Fedorov A, Beichel R, Kalpathy-Cramer J, et al. 3D Slicer as an image computing platform for the Quantitative Imaging Network. Magn Reson Imaging 2012;30:1323–41. https://doi.org/10.1016/j.mri.2012.05.001.
[46] Velazquez ER, Parmar C, Jermoumi M, et al. Volumetric CT-based segmentation of NSCLC using 3D-Slicer. Sci Rep 2013;3:3529. https://doi.org/10.1038/srep03529.
[47] Casanueva FF, Barkan AL, Buchfelder M, et al. Criteria for the definition of Pituitary Tumor Centers of Excellence (PTCOE): a pituitary society statement. Pituitary 2017;20:489–98. https://doi.org/10.1007/s11102-017-0838-2.
[48] Cazabat L, Dupuy M, Boulin A, et al. Silent, but not unseen: multimicrocystic aspect on T2-weighted MRI in silent corticotroph adenomas. Clin Endocrinol (Oxf) 2014;81:566–72. https://doi.org/10.1111/cen.12443.
[49] Potorac I, Beckers A, Bonneville J-F. T2-weighted MRI signal intensity as a predictor of hormonal and tumoral responses to somatostatin receptor ligands in acromegaly: a perspective. Pituitary 2017;20:116–20. https://doi.org/10.1007/s11102-017-0788-8.
*[50] Heck A, Emblem KE, Casar-Borota O, et al. Quantitative analyses of T2-weighted MRI as a potential marker for response to somatostatin analogs in newly diagnosed acromegaly. Endocrine 2016;52:333–43. https://doi.org/10.1007/s12020-015-0766-8.
[51] Rogg JM, Tung GA, Anderson G, et al. Pituitary apoplexy: early detection with diffusion-weighted MR imaging. AJNR Am J Neuroradiol 2002;23:1240–5.
[52] Kunii N, Abe T, Kawamo M, et al. Rathke's cleft cysts: differentiation from other cystic lesions in the pituitary fossa by use of single-shot fast spin-echo diffusion-weighted MR imaging. Acta Neurochir (Wien) 2007;149:759–69. https://doi.org/10.1007/s00701-007-1234-x.
[53] Pierallini A, Caramia F, Falcone C, et al. Pituitary macroadenomas: preoperative evaluation of consistency with diffusion-weighted MR imaging—initial experience. Radiology 2006;239:223–31. https://doi.org/10.1148/radiol.2383042204.
[54] Wang M, Liu H, Wei X, et al. Application of reduced-FOV diffusion-weighted imaging in evaluation of normal pituitary glands and pituitary macroadenomas. AJNR Am J Neuroradiol 2018;39:1499–504. https://doi.org/10.3174/ajnr.A5735.
[55] Yiping L, Ji X, Daoying G, et al. Prediction of the consistency of pituitary adenoma: A comparative study on diffusion-weighted imaging and pathological results. J Neuroradiol 2016;43:186–94. https://doi.org/10.1016/j.neurad.2015.09.003.
[56] Mahmoud OM, Tominaga A, Amatya VJ, et al. Role of PROPELLER diffusion-weighted imaging and apparent diffusion coefficient in the evaluation of pituitary adenomas. Eur J Radiol 2011;80:412–7. https://doi.org/10.1016/j.ejrad.2010.05.023.
[57] Sanei MT, Kimia F, Mehrnahad M, et al. Accuracy of diffusion-weighted imaging-magnetic resonance in differentiating functional from non-functional pituitary macro-adenoma and classification of tumor consistency. Neuroradiol J 2019;32:74–85. https://doi.org/10.1177/1971400918809825.
[58] Suzuki C, Maeda M, Hori K, et al. Apparent diffusion coefficient of pituitary macroadenoma evaluated with line-scan diffusion-weighted imaging. J Neuroradiol 2007;34:228–35. https://doi.org/10.1016/j.neurad.2007.06.007.
[59] Yu CS, Li KC, Xuan Y, et al. Diffusion tensor tractography in patients with cerebral tumors: a helpful technique for neurosurgical planning and postoperative assessment. Eur J Radiol 2005;56:197–204. https://doi.org/10.1016/j.ejrad.2005.04.010.
[60] Salmela MB, Cauley KA, Nickerson JP, et al. Magnetic resonance diffusion tensor imaging (MRDTI) and tractography in children with septo-optic dysplasia. Pediatr Radiol 2010;40:708–13. https://doi.org/10.1007/s00247-009-1478-0.
[61] Anik I, Anik Y, Cabuk B, et al. Visual outcome of an endoscopic endonasal transsphenoidal approach in pituitary macroadenomas: quantitative assessment with diffusion tensor imaging early and long-term results. World Neurosurg 2018;112:e691–701. https://doi.org/10.1016/j.wneu.2018.01.134.
[62] Ma Z, He W, Zhao Y, et al. Predictive value of PWI for blood supply and T1-spin echo MRI for consistency of pituitary adenoma. Neuroradiology 2016;58:51–7. https://doi.org/10.1007/s00234-015-1591-8.
[63] Bladowska J, Zimny A, Guziński M, et al. Usefulness of perfusion weighted magnetic resonance imaging with signal-intensity curves analysis in the differential diagnosis of sellar and parasellar tumors: preliminary report. Eur J Radiol 2013;82:1292–8. https://doi.org/10.1016/j.ejrad.2013.01.033.
[64] Hakyemez B, Yildirim N, Erdoğan C, et al. Meningiomas with conventional MRI findings resembling intraaxial tumors: can perfusion-weighted MRI be helpful in differentiation? Neuroradiology 2006;48:695–702. https://doi.org/10.1007/s00234-006-0115-y.
[65] Manara R, Maffei P, Citton V, et al. Increased rate of intracranial saccular aneurysms in acromegaly: an MR angiography study and review of the literature. J Clin Endocrinol Metab 2011;96:1292–300. https://doi.org/10.1210/jc.2010-2721.
[66] Linn J, Peters F, Lummel N, et al. Detailed imaging of the normal anatomy and pathologic conditions of the cavernous region at 3 Tesla using a contrast-enhanced MR angiography. Neuroradiology 2011;53:947–54. https://doi.org/10.1007/s00234-011-0837-3.
[67] Hughes JD, Fattahi N, Van Gompel J, et al. Magnetic resonance elastography detects tumoral consistency in pituitary macroadenomas. Pituitary 2016;19:286–92. https://doi.org/10.1007/s11102-016-0706-5.
[68] Pînzariu O, Georgescu B, Georgescu CE. Metabolomics—a promising approach to pituitary adenomas. Front Endocrinol (Lausanne) 2019;9:814. https://doi.org/10.3389/fendo.2018.00814.
[69] Chernov MF, Kawamata T, Amano K, et al. Possible role of single-voxel 1H-MRS in differential diagnosis of suprasellar tumors. J Neurooncol 2009;91:191–8. https://doi.org/10.1007/s11060-008-9698-y.
[70] Sutton LN, Wang ZJ, Wehrli SL, et al. Proton spectroscopy of suprasellar tumors in pediatric patients. Neurosurgery 1997;41:388–94. discussion 394–5.
[71] Hu J, Yan J, Zheng X, et al. Magnetic resonance spectroscopy may serve as a presurgical predictor of somatostatin analog therapy response in patients with growth hormone-secreting pituitary macroadenomas. J Endocrinol Invest 2019;42:443–51. https://doi.org/10.1007/s40618-018-0939-4.

[72] Lang M, Habboub G, Moon D, et al. Comparison of constructive interference in steady-state and T1-weighted MRI sequence at detecting pituitary adenomas in Cushing's disease patients. J Neurol Surg Part B Skull Base 2018;79:593–8. https://doi.org/10.1055/s-0038-1642032.
[73] Yamamoto J, Kakeda S, Shimajiri S, et al. Tumor consistency of pituitary macroadenomas: predictive analysis on the basis of imaging features with contrast-enhanced 3D FIESTA at 3T. Am J Neuroradiol 2014;35:297–303. https://doi.org/10.3174/ajnr.A3667.
[74] Watanabe K, Kakeda S, Yamamoto J, et al. Delineation of optic nerves and chiasm in close proximity to large suprasellar tumors with contrast-enhanced FIESTA MR imaging. Radiology 2012;264:852–8. https://doi.org/10.1148/radiol.12111363.
[75] Chatain GP, Patronas N, Smirniotopoulos JG, et al. Potential utility of FLAIR in MRI-negative Cushing's disease. J Neurosurg 2018;129:620–8. https://doi.org/10.3171/2017.4.JNS17234.